CLOSE-RANGE STEREO REGISTRATION FOR CONCRETE CRACK MONITORING

M. NAKAGAWA, F. KATUKI, Y. ISOMATU and T. KAMADA

Department of Civil Engineering, College of Engineering, Shibaura Institute of Technology, Japan

ABSTRACT

In monitoring concrete cracks over time, there is a geometrical transformation of the concrete surfaces as the cracks progress. Thus, tracking structural deterioration requires conducting reference point measurements with every 3D measurement. We propose a temporal 3D data registration methodology based on the iterative closest-point algorithm. We conducted an indoor experiment to clarify the progress of structure deterioration. Our experimental results confirm the validity of our approach.

Keywords: concrete crack monitoring, photogrammetry, close-range stereo, 3D data registration.

1. INTRODUCTION

Cameras can record objective data in daily structure maintenance. In particular, close-range photogrammetry can provide geometric images using a stereo camera for structures. Generally, close-range photogrammetry requires reference points on the measured surfaces to generate 3D data with camera orientation estimation. Single cameras and stereo cameras using reference points have been used in concrete crack tracking in conventional approaches (Abdel-Qader et al. 2003; Hutchinson et al. 2006; Yamaguchi et al. 2008). However, for periodical concrete crack monitoring, the concrete surface is geometrically transformed as the cracks progress. This geometrical transformation is a primary cause of image registration error. Thus, to follow structure deterioration, we must conduct a reference point measurement using survey instruments, such as a Total Station, in each 3D measurement. Thus, we propose a temporal 3D data registration methodology based on the iterative closest-point algorithm without reference point measurements. We also confirm that a fixed baseline stereo camera can perform periodic concrete crack monitoring without known reference points or external orientation. Avoiding external orientation allows a significant improvement in the efficiency of infrastructure monitoring. Finally, we present experimental results that confirm the validity of our approach.

2. METHODOLOGY

Our proposed process flow is shown in Figure 1. We use a fixed-baseline stereo camera to avoid the requirement for known reference points. After stereo calibration, the fixed-baseline stereo cameras can acquire 3D data as the environment changes without periodic external orientation. Next, corresponding points are extracted from each temporal stereo image to estimate the 3D data using a stereo-matching procedure. Then, tie-points are extracted from the periodic scenes using the estimated 3D data. The acquired periodic 3D data are then registered using the extracted tie-points. The registration consists of a preliminary registration (camera rotation and translation) and iterative registration. Generally, there is geometric distortion in the tie-point distribution in temporal images because of the transformation of the concrete surfaces. However, this distortion can be averaged using iterative registration with distributed tie-points. Thus, even if there is a transformation on the concrete surface, precise registration is still possible. Finally, concrete crack progress can be observed following periodic 3D data registration.

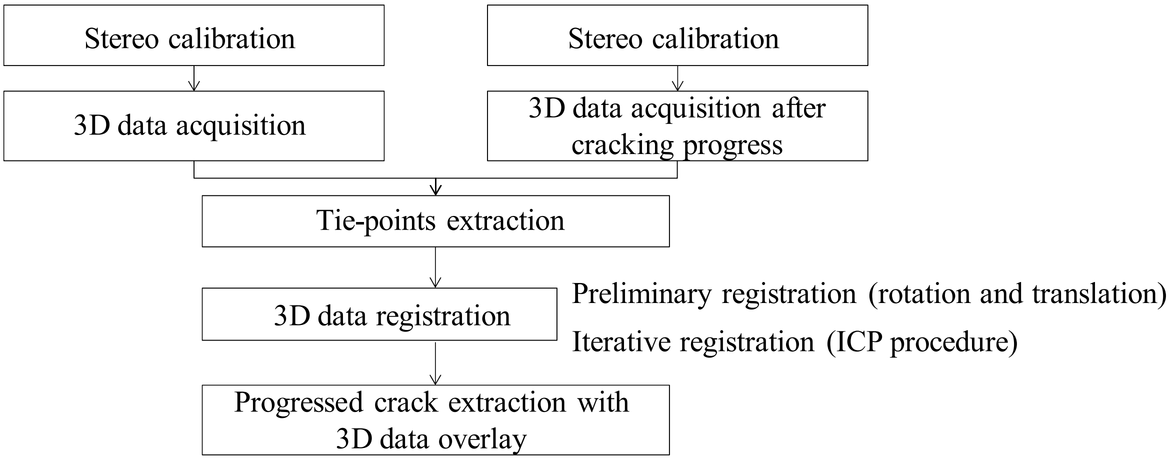

Figure 1: Proposed processing flow.

2.1. Stereo calibration

We applied Zhang's calibration approach (Zhang 2000) to our fixed baseline stereo. This approach estimates interior camera parameters using projection transformation parameters into multiple planes. The projection transformation can represent a plane translation in a perspective projection model. First, a linear constrained equation is formulated in which the constraint satisfies a recorded orthonormal basis between projective transformation matrices. Next, initial values are estimated using the closed-form solution algorithm analytically. Then, estimated parameters are improved with the Levenberg-Marquardt algorithm. Specifically, we minimize the following Equation (1) to estimate interior parameters ($\mathbf{A}$, k_1, k_2) and external parameters ($\mathbf{R}_i$, $\mathbf{t}_i$).

$$\sum_{i=1}^{n}\sum_{j=1}^{m}\|\mathbf{m}_{ij}-\breve{\mathbf{m}}(\mathbf{A},k_1,k_2,\mathbf{R}_i,\mathbf{t}_i,\mathtt{M}_j)\|^2 \qquad (1)$$

2.2. 3D data registration

First, periodic 3D data are generated by stereo matching using the stereo images acquired by the fixed baseline stereo cameras and registered using the periodic tie-points extracted from each stereo image. The registration of periodical 3D data is equivalent to 3D point cloud integration. The iterative closest-point (ICP) algorithm (Rusinkiewicz and Levoy 2000) is the most advantageous approach to integration of 3D point cloud for procedures such as terrestrial laser scanning and simultaneous localization and mapping (Durrant-Whyte and Bailey 2006). Generally, the ICP algorithm provides a correspondence between two groups (X and Y) of point data. In the first step, a temporal correspondence is formed between the two groups as initial values. For example, we estimate the nearest point $\boldsymbol{y_i}$ in the group Y from a point $\boldsymbol{x_i}$ in the group X. In the second step, Equation (2) is minimized to estimate rotation and translation parameters. These procedures are then iterated until the rotation and translation parameters are fixed.

$$\min \sum_i \|\boldsymbol{y_i} - (R\boldsymbol{x_i} + \boldsymbol{t})\|^2 \qquad (2)$$

When corresponding points exist in point groups X and Y, the centers of gravity of the point groups also correspond. Equation (2) is transformed to an equation with $\boldsymbol{t}$ eliminated by translations of the two groups. Thus, a rotation and translation parameter estimation becomes a rotation matrix R estimation, using an approach, such as singular value decomposition (SVD), eigenvector orthogonal matrix, or quaternions; the estimation accuracies of these approach are almost the same. We applied the SVD approach to estimate the rotation matrix R. Registered periodic 3D data are projected into a plane including the concrete crack to generate periodic ortho images. These ortho images can provide efficiency improvement in visual inspections for users. Moreover, conventional feature extraction algorithms using 2D images can be used to detect a concrete crack automatically.

3. EXPERIMENT

A test object was measured using a fixed baseline stereo at closed range. Next, acquired 3D data were registered using the ICP algorithm from periodic stereo images with unknown targets. Finally, progress was monitored using the registered data.

First, a reinforced concrete beam was prepared as the test object. It had a hexagonal shape and was 120 cm long, 10 cm wide, and 15 cm high. The beam included steel fibers to improve its structure against a shearing stress, and to facilitate flexural cracking. Next, the fixed baseline stereo system was assembled to satisfy 3D measurement accuracy within 0.1 mm to recognize crack progression without known reference points for external orientation; details are shown in Table 1.

Table 1: Stereo camera configuration

Camera configuration			Stereo configuration	
Camera	Nikon D300		Camera baseline	15 cm
Image size	2144 × 1424 pix		Measurement distance	70 cm
Focul length	35 mm		3D measurement accuracy	0.033 mm

We then simulated a periodic concrete structure investigation in the indoor experiment shown in Figure 2. The beam was first moved to a loading station and loaded to generate or progress a crack. We then released the load from the beam after crack generation or progress, and moved the beam to the image-acquisition position, and a stereo image was acquired. We repeated the process five times, in STEP1 to STEP5, as shown in Figure 3. Loading logs and visual crack measurement logs after each loading are shown in Table 2.

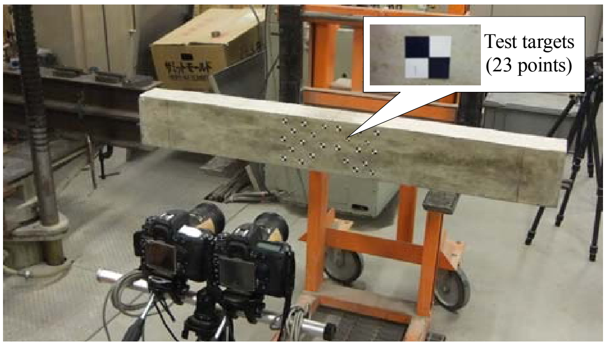

Figure 2: Experimental environment.

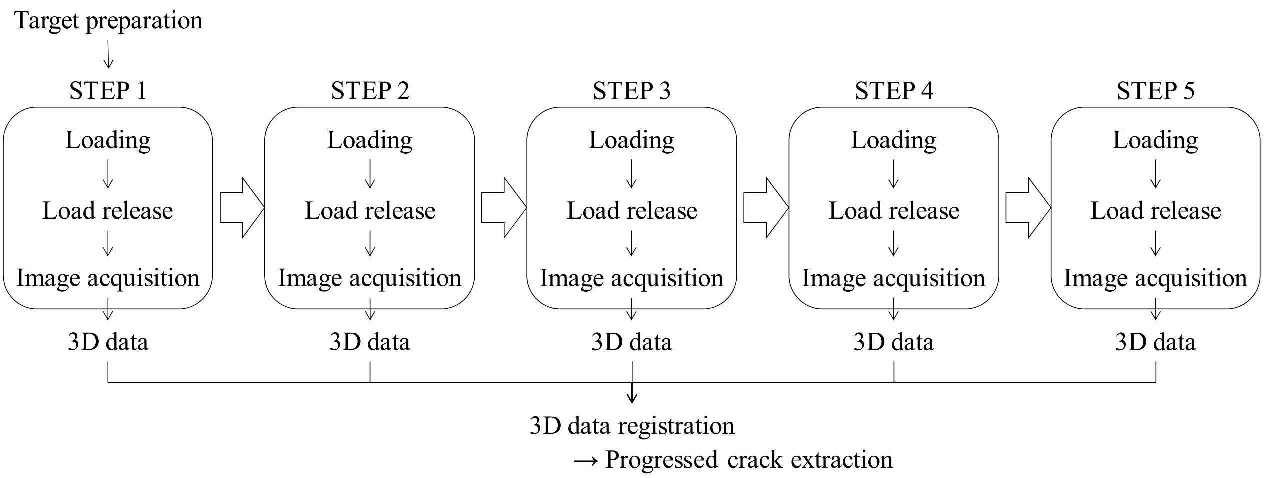

Figure 3: Measurement sequence.

Table 2: Visual measurement results and loading log

Loading step	STEP 1	STEP 2	STEP 3	STEP 4	STEP 5
Maximum load [kN]	9.0	11.0	13.0	13.0	13.2
Maximum crack width after loading [mm]		～0.05	0.15	0.30	0.70
Crack length after loading [cm]		8.2	10.8	11.9	12.2

We also pasted 23 sheet targets as unknown targets on the surface of the object. The unknown targets were measured with the fixed baseline stereo after stereo calibration. We then set 57 verification baselines with Delaunay division using the targets, as shown in Figure 4.

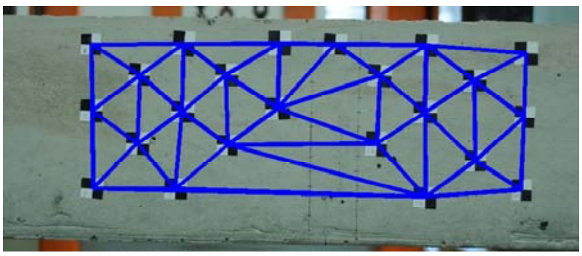

Figure 4: Verification baselines drawn using Delaunay division.

Additionally, tie-points were acquired from the targets in temporal images using a semi-automated procedure to monitor the periodic displacement of the target arrangement for a confirmation of the geometrical transform on the concrete surface after the crack progress. Then, we conducted a verification baseline measurement and periodic ortho image generation using temporal stereo images to evaluate our ICP registration performance.

4. RESULTS

4.1. Baseline verification using close-range stereo

Relative 3D displacements were measured with the stereo cameras using verification baselines, as shown in Figure 5. Our verification baseline measurement results are shown in Figure 6. The wide red lines indicate 3D displacements longer than 0.15 mm on the verification baselines. Additionally, displacements of each maximum crack width from STEP3 to STEP5 are shown in Table 3.

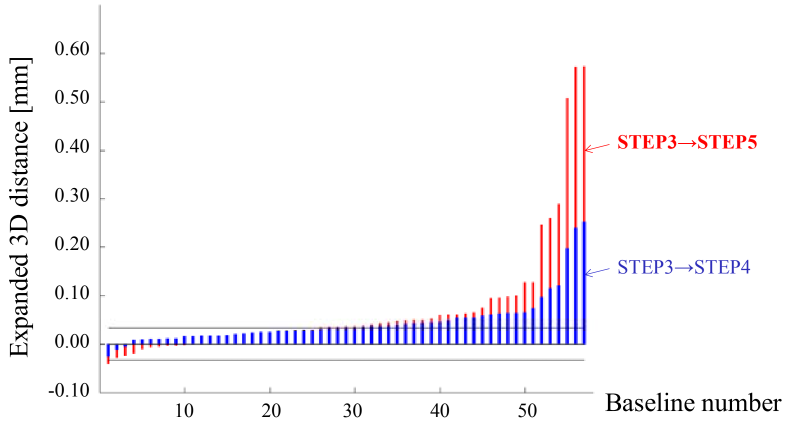

Figure 5: Relative 3D displacements on verification baselines.

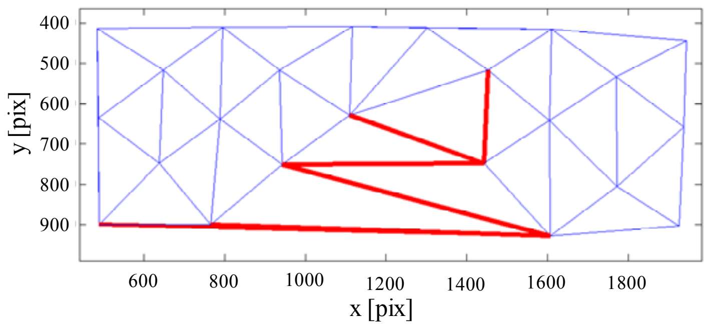

Figure 6: Verification baselines that show relative 3D displacements greater than 0.15 mm.

Table 3: Comparison of visual measurement results with stereo measurement results

	STEP3→STEP4	STEP3→STEP5
Visual measurement result	0.15 mm	0.55 mm
Stereo measurement result	0.217 mm	0.536 mm

4.2. ICP registration

We registered 3D data between STEP3 and STEP4, and between STEP3 and STEP5. These registration results are shown in Table 4.

Table 4: Results of ICP registration

	STEP3→STEP4	STEP3→STEP5
Average values of 3D distance between corresponded points	0.103 mm	0.191 mm
Standard deviation values 3D distance between corresponded points	0.050 mm	0.104 mm

4.3. Periodical ortho-image generation

Ortho images using periodic stereo were projected onto a plane on measured surfaces, as shown in Figure 7. The spatial resolution was 0.2 mm, and the projection accuracy was 1 pixel.

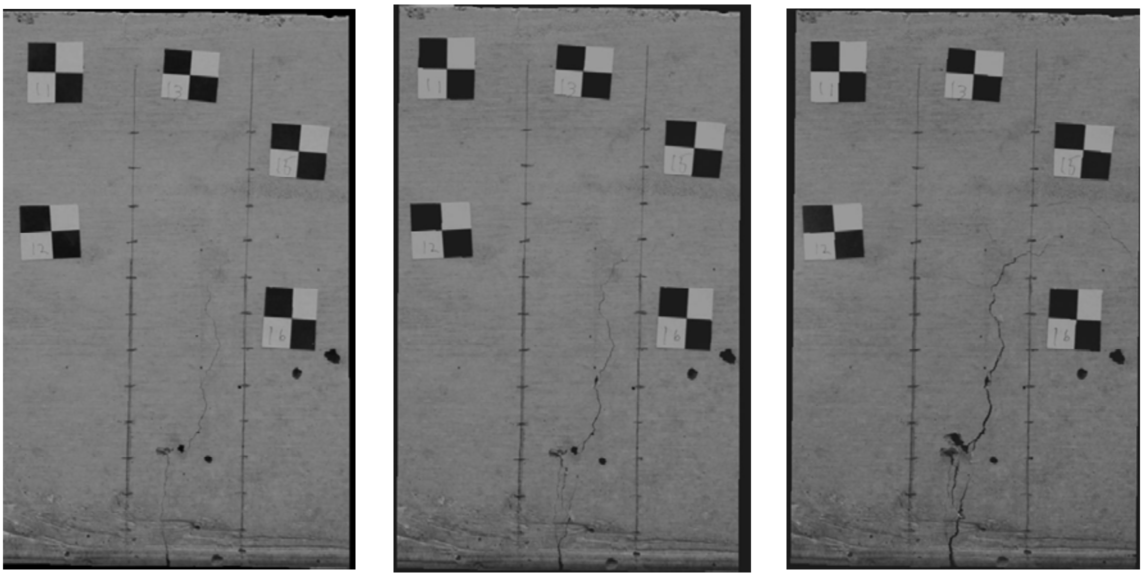

Figure 7: Ortho images (left image: projected result in STEP3, center image: projected result in STEP4, and right image: projected result in STEP5).

5. DISCUSSION

5.1. Stereo measurement and ICP registration

We confirmed that a concrete crack occurred at the same position in the visual measurement results and stereo measurement results, as shown in Figure 6. In Figure 5, Figure 6, and Table 3, we also confirmed a periodic transformation caused by crack progression from 0.2 mm to 0.5 mm on the concrete surface. In Table 4, we also confirmed that ICP registration achieved high registration accuracy, from 0.1 mm to 0.2 mm, even if the reference points move on the measured objects. These results indicate that our approach can achieve precise 3D data registration when there is a transformation on the concrete surface.

5.2. Concrete crack extraction

The spatial resolution of ortho image projection was 0.2 mm. Thus, concrete cracks less than 0.2 mm in width were not clear in the image. However, subpixel image estimation can improve the spatial resolution virtually, including the pointing accuracy in an image. Moreover, a pointing result (an image coordinate value in an ortho image) refers to a 3D coordinate value in the point cloud data automatically. Thus, when we trace a crack in the ortho image, we can trace 3D coordinate values with 0.033 mm accuracy, as well as the stereo measurement accuracy in our experiment. In preliminary experiments, we confirmed that each section of a concrete crack can be measured with a feature extraction procedure using a distance value added to the ortho image (Verbree et al. 2005), as shown in Figure 8.

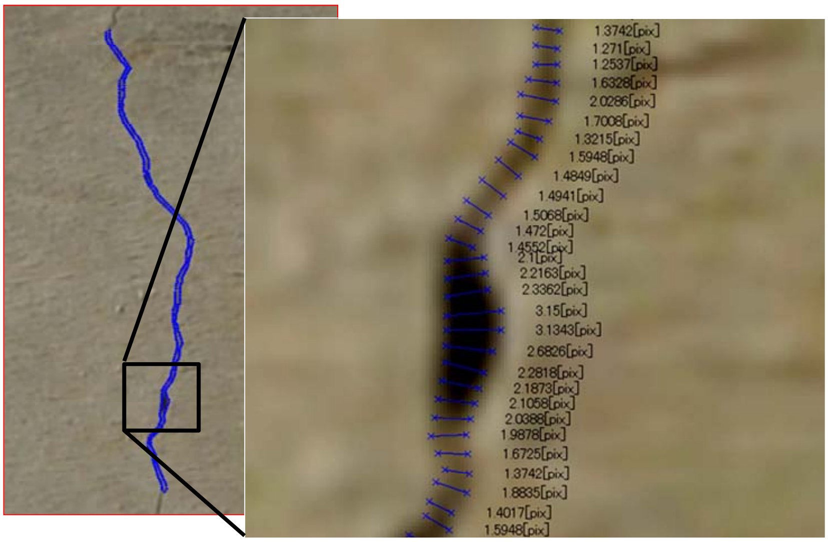

Figure 8: Automated crack extraction result.

5.3. Point cloud data generation with stereo matching

Figure 9 shows the results of point cloud generation using stereo images. This figure shows that fixed baseline stereo can generate 3D data even if the reference point coordinate values are unknown.

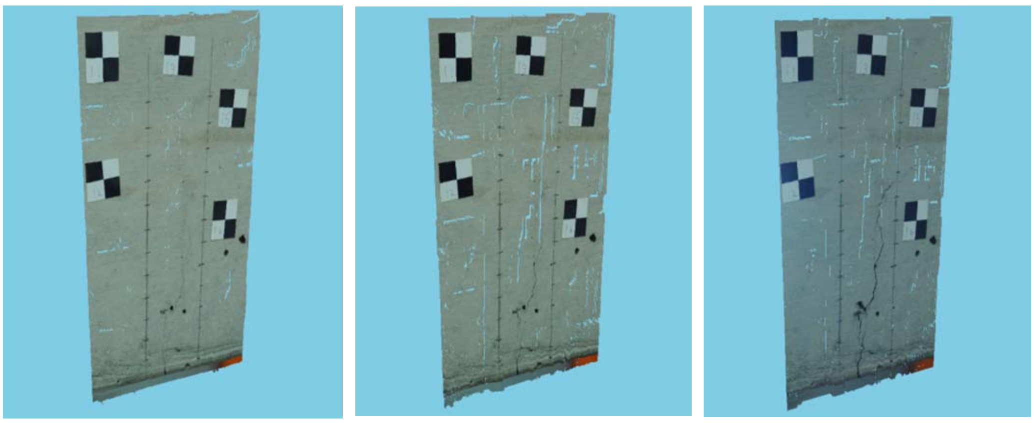

Figure 9: Point cloud generation results using close-range stereo (left image: point cloud after STEP3, center image: point cloud after STEP4, and right image: point cloud after STEP5).

We applied coarse-to-fine image matching using a spatial constraint with iterative surface model generation (Nakagawa et al. 2011) and point cloud visualization (Nakagawa 2011) to generate point clouds using stereo images.

6. CONCLUSIONS

We have proposed a temporal 3D data registration methodology based on the iterative closest point algorithm without additional measurements of reference points. We confirmed that fixed baseline stereo cameras can perform periodic concrete crack monitoring without known reference points or external orientation. Finally, we have presented experimental results that confirm the validity of our approach. Thus, even when there is a geometrical transformation on concrete surfaces in periodic concrete crack monitoring, our results suggest that the periodic 3D crack data can be registered to investigate crack progression. However, it is necessary to clarify the following issues in future work. The first issue is the minimum number of targets to maintain 3D data registration accuracy. The second issue is a suitable arrangement of unknown reference targets. The third issue is a development of 3D registration methodology without reference markers.

REFERENCES

Ikhlas Abdel-Qader, Osama Abudayyeh, and Michael E. Kelly (2003). Analysis of edge detection techniques for crack identification in bridges. Journal of Computing in Civil Engineering 2003, 17(3), pp.255–263.

Tara C. Hutchinson and ZhiQiang Chen (2006). Improved image analysis for evaluating concrete damage. Journal of Computing in Civil Engineering 2006, 20(3), pp.210–216.

Tomoyuki Yamaguchi, Shingo Nakamura, Ryo Saegusa and Shuji Hashimoto (2008). Image-Based Crack Detection for Real Concrete Surfaces. IEEJ Transactions on Electrical and Electronic Engineering, Volume 3, Issue 1, pp.128–135.

Zhengyou Zhang (2000). A Flexible New Technique for Camera Calibration. IEEE Transactions on Pattern Analysis and Machine Intelligence, 22(11):1330–1334.

Szymon Rusinkiewicz and Marc Levoy (2001). Efficient Variants of the ICP Algorithm. Third International Conference on 3D Digital Imaging and Modeling (3DIM), pp.145-152.

Hugh Durrant-Whyte and Tim Bailey (2006). Simultaneous localization and mapping (SLAM): part I. Robotics & Automation Magazine, IEEE, Vol. 13, Issue: 2, pp. 99-110.

Tim Bailey and Hugh Durrant-Whyte. (2006). Simultaneous localization and mapping (SLAM): part II. Robotics & Automation Magazine, IEEE, Vol. 13, Issue: 3, pp. 108-117.

Edward Verbree, Sisi Zlatanova, and Sander Dijkman (2005). Distance-value-added panoramic images as the base data model for 3D-GIS. Panoramic Photogrammetry Workshop.

Masafumi Nakagawa (2011). LiDAR VR generation with point-based rendering. The Urban Data Management Society Symposium 2011, Vol.XXXVIII, pp. 223-230.

Masafumi Nakagawa, Anna Nakanishi, Hirotaka Endo, and Kenta Ochiai (2011). Massive Point Cloud Acquisition on a Soil Surface Using a Stereo Camera. GEOMAT2011 (International Conference on Geotechnique, Construction Materials and Environment) , pp.421-424.